Anisotropy of the proton kinetic energy in ice Ih

Y. Finkelstein,[1*] R. Moreh,[2] F. Bianchini,[3] and P. Vajeeston[3]

[1] Chemistry Division, Nuclear Research Center Negev (NRCN), Beer-Sheva 84190, Israel

[2] Physics Department, Ben-Gurion University of the Negev, Beer-Sheva 84105, Israel

[3] Center for Materials Sciences and Nanotechnology, Department of Chemistry, University of Oslo, N-0315 Oslo, Norway

Abstract

The partial vibrational density of states (pVDOS) of ice Ih, as simulated by first principle modeling based on density functional theory (DFT), is utilized for computing the Cartesian components of the proton and oxygen quantum kinetic energies, Ke(H) and Ke(O) respectively, along and perpendicular to the hydrogen bonds. The DFT method was found to yield better agreement with deep inelastic neutron scattering (DINS) measurements than the semi empirical (SE) calculations. The advantage of using the DFT method is to enable us to resolve the external and internal phonon bands of the Cartesian projections of the pVDOS, and hence those of the lattice and vibrational components of Ke(H). We show that a pVDOS analysis is a valuable tool in testing scattering results of complex systems and suggest its potential to explore competing quantum effects, e.g. on Ke(H) across phase transitions in water.

Introduction

A substantial body of experimental work exists on the nuclear nuclear kinetic energy of the proton, Ke(H), in ice and water. Only one scattering technique, namely deep inelastic neutron scattering (DINS), was utilized for measuring Ke(H) in H_2O phases. Out of those, DINS is regarded as the only standard method for *direct* Ke(H) determinations of the proton zero point kinetic energy (ZPKE), via a measure of the proton radial momentum distribution (RMD). Note that the kinetic energy of the H-atom in H_2O up to ~ 280 K is practically equal to its ZPKE.[1] Currently, measuring the ZPKE is provided only by the Vesuvio spectrometer at ISIS (Rutherford Appleton Laboratory, UK). Worth mentioning in that regard, is that Ke(H) may also be determined by inelastic neutron scattering (INS).[2] Significantly different from DINS however, in INS one measures the fundamental frequencies of the condensed

H_2O phase. These INS data are normally used as input for calculating Ke(H) in the semi empirical (SE) method in which the harmonic approximation (HA) is assumed.[3]

Lately, an extensive experimental and theoretical emphasis is given in the literature for measuring and computing the Cartesian components of Ke(H) along and perpendicular to the hydrogen bond (HB) direction in H_2O.[2,4,5,6,7,8,9] These components and were found to provide a direct estimate of competing quantum effects (CQEs).[5] By now, such components in light water in the form of ice Ih were measured directly only by DINS[2,8] and calculated semi empirically by utilizing INS measurements.[2]

In the present work we report on the first DFT simulation of the Cartesian components of the H-VDOS in ice Ih from which the directional components of Ke(H) along and perpendicular to the hydrogen bond are resolved. It is encouraging that the currently deduced values are in good agreement with available measured DINS data on solid H_2O, a result which emphasizes the validity of the pVDOS approach as a powerful tool in exploring proton dynamics of HB containing systems.

Theoretical Remarks

In the following we emphasize the advantages of using a *p*VDOS analysis over the SE approach for treating the directional Ke(H) in ice.

***p*VDOS vs SE**

The SE approach.[2,3,1] is used to compute Ke(H) in condensed H_2O phases where it is assumed that the coupling of the H_2O modes of motion to the HBs network is fully accounted for by utilizing the *measured* frequencies of H_2O and its geometric parameters (R_{OH} and the HOH angle). For H_2O, five discrete frequencies exist arising from the two lattice modes (translation and libration of the entire H_2O molecule) and from its three internal vibrations (OHO bending and two OH stretching modes). Theses frequencies are then reconstructed by solving the equations of motion of the oxygen atom and two protons of H_2O. This procedure yields the atomic amplitudes along any direction, thus providing the energy fractions shared by the constituent atom in each mode of motion along any direction. These fractions are used to deduce the Cartesian XYZ components of Ke(H) and Ke(O).

The SE approach was found to work flawlessly as it successfully predicted DINS Ke(H,D,O) values in various phases of $H(D)_2$ and $H(D)_2O$.[10,11] In fact, it was established as a powerful

tool for predicting atomic KE values (already way back in the 70th/90th) of $^{15}N/^{13}C$, contained in a variety of molecular systems; the results were in excellent agreement with nuclear resonance photon scattering/fluorescence (NRPS/NRF) experiments.[12,13,14,15,16,17]

It is also very interesting to note that despite the fact that the SE method relies on the HA, it was found to be applicable to cases involving strong anharmonic potentials.[18] Examples include:[18] ferroelectric crystals of the KDP family (MH_2PO_4; M = K, Rb, Cs), and the super protonic conductor $Rb_3H(SO_4)_2$ in which HB symmetrization is very nearly realized. In such systems, it is necessary to account for the pVDOS, i.e. the part of the VDOS shared by the protons (H-VDOS), as simulated by DFT or molecular dynamics (MD).[18] Note that the *p*VDOS approach is more accurate than the SE method as it accounts for both the continuous phonon distribution of the system and for the fraction shared by the proton in all vibrational states (phonons). Moreover, the energy fractions distribution is self-contained in the *p*VDOS and it is unnecessary to calculate it in advance as in the SE approach.

A breakdown of the SE approach in predicting Ke(H) values was first demonstrated in DINS studies of *nanoconfined* H_2O where anomalous Ke(H) deviations of ± 30-50 % (from the standard value of Ke(H) ~ 152 meV measured in e.g. ice) were reported. These were found in cases such as protein hydration shell water[19] and in water nanoconfined in silica gels,[20,21] in carbon nanotubes[22] and in Beryl.[23] These anomalies couldn't be captured however by the SE approach nor by more sophisticated theoretical calculations such as path integral molecular dynamics (PIMD)[24,25,26] and path integral monte Carlo (PIMC)[27,28,29,26] calculations. Only very recently, a first success was reported by utilizing first principle based DFT simulations of the *partial* H-VDOS in the H_2O@Berryl system.[30] By treating the whole system, of the hosting Beryl lattice and the confined H_2O, as a single quantum system, the deduced Ke(H) at 5K was found to conform precisely to the DINS measured anomalous value, Ke(H) = 104 meV.[23] The key insight here is that under nano-confinement, the coupling of the water molecule to host lattice modes yield proton states distinctly different from those of ordinary water phases.[31] This success was in fact the first accurate theoretical reconstruction of an anomalous DINS Ke(H) value in nanoconfined water, by which the crucial importance of the coupling of the water modes of motion to host lattice modes in calculating KEs was realized .

SE calculation

In the following we stick to the notation of Ref. [2] by selecting the direction of OH1 covalent bond to be the same as the Z Cartesian direction and along the HB direction in ice Ih. The relative directions of the abc crystallographic axes and the Cartesian XYZ ones are defined in Fig. 1.
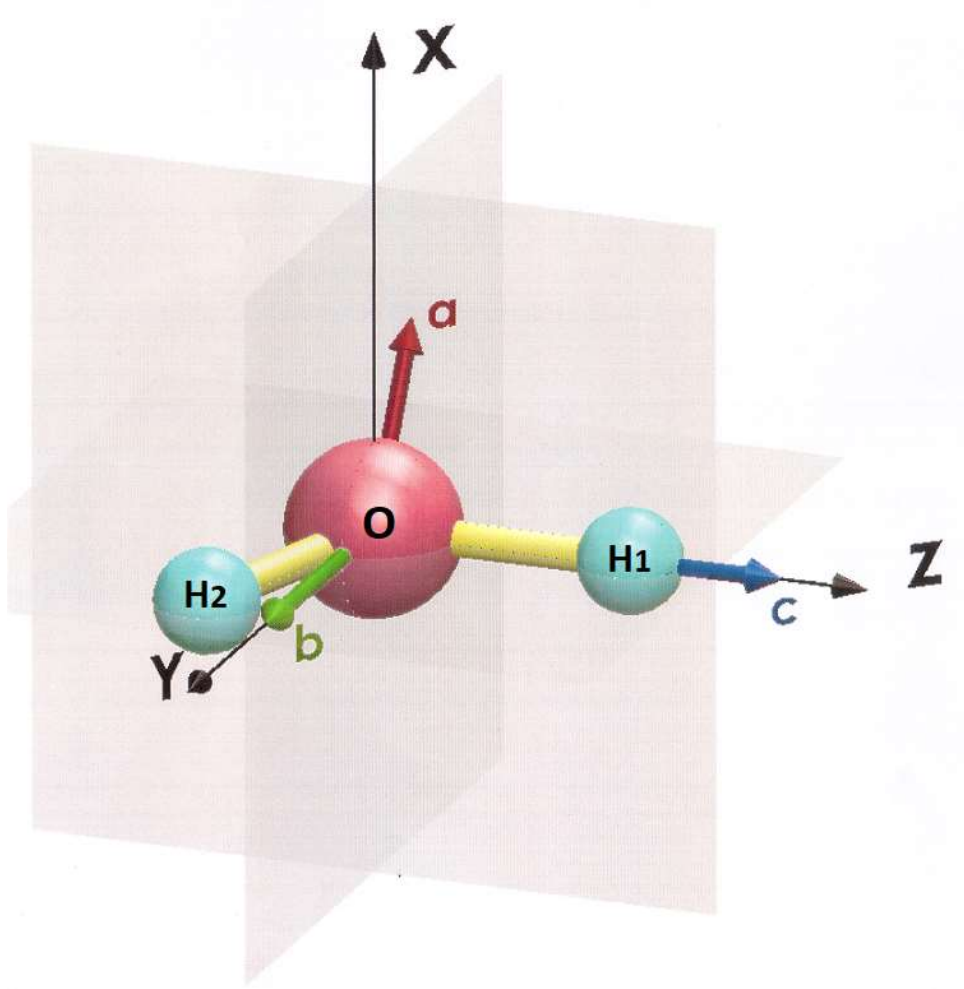
Fig. 1 Definition of the XYZ Cartesian directions in H_2O: the OH_1 covalent bond is along z, and the (Y,Z) plane coincides with the H_2O molecular plane. The relation of the Cartesian axes frame to the abc crystallographic one of hexagonal ice (see Fig. 2), is also shown: c$\|$Z, (b,c)$\|$(Y,Z), b$\perp$c, a$\perp$c, $\angle ab = 120°$ ($\angle aX = 30°$, $\angle Yb \sim 17°$).

Accounting for the directions defined in Fig. 1, the following relations apply to the H_1 atom:[2,32]

$$Ke_x(H_1) = S_t\alpha(\upsilon_t) + (S_{Ry}+S_{Rz})\alpha(\upsilon_R) \qquad\qquad (1)$$

$$Ke_y(H_1) = S_t\alpha(\upsilon_t) + S_{Rx}\alpha(\upsilon_R) + S_2\alpha(\upsilon_2) \qquad\qquad (2)$$

4

$Ke_z(H_1) = S_t\alpha(\upsilon_t) + S_1\alpha(\upsilon_1) + S_3\alpha(\upsilon_3)$ (3)

S_t, $S_{Rx,y,z}$, $S_{1,2,3}$ are the KE fractions shared by H_1 in the translational, rotational (around the Cartesian axes passing through the molecular center of mass) and the three internal frequencies of H_2O respectively. $\alpha(\upsilon_j) = \dfrac{h\upsilon_j}{2}\left(\dfrac{1}{e^{\frac{h\upsilon_j}{kT}}-1} + \dfrac{1}{2}\right)$, is the KE of the corresponding Planck oscillator, with υ_j (j = t, r, bnd, ss, as) the *measured* characteristic frequency of translation, libration and three internal (bending and symmetric and asymmetric stretch) modes of motion of H_2O. It should be noted that in this simplified model, one accounts in each mode for the same characteristic frequency (measured for the studied water phase) regardless of the direction, thus coupling effects of the water molecule to surrounding lattice modes are ignored.

*p*VDOS calculation

A detailed discussion of the KE calculation by the *p*VDOS method may be found elsewhere.[18] Here we just mention that by accounting for the lth Cartesian component (l = X, Y, Z) of the H-VDOS, $g_{H_l}(\nu)$, the directional component of Ke(H), $Ke_l(H)$, may be deduced directly by:

$$Ke_l(H) = \frac{\frac{3}{2}\int_{\nu_0}^{\nu_f} g_{H_l}(\nu)\alpha(\nu,T)d\nu}{\int_{\nu_0}^{\nu_f} g_{H_l}(\nu)d\nu}$$ (4)

with ν_0 and ν_f the frequency limits of $g_{H_l}(\nu)$.

DFT simulation of $g_{H_l}(\upsilon)$

Total energies have been calculated using the projected-augmented plane-wave (PAW) implementation of the Vienna *ab initio* simulation package (VASP).[33,34] All these calculations were made with the Perdew, Burke, and Ernzerhof (PBE)[35] exchange correlation functional. Ground-state geometries were determined by minimizing stresses and Hellman-Feynman forces using the conjugate-gradient algorithm with a force convergence threshold of 10^{-3}eV Å^{-1}. Brillouin zone integration was performed with a Gaussian broadening of 0.1 eV. From various sets of calculations it was found that 512 **k** points in the Brillouin zone and a 600 eV plane-wave cut-off are sufficient to ensure optimum accuracy in the computed

results. The **k**-points were generated using the Monkhorst-Pack method with a grid size of 8×8×8.

A frozen phonon calculation was performed on suitably large supercells using the Phonopy program to obtain the phonon dispersion curve and density of states.[36] An atomic displacement of 0.0075 Å was used with a symmetry consideration to obtain the force constants for the phonon calculations. The displacements in opposite directions along all possible axes were included in the calculations to improve the overall accuracy. The forces are calculated using the VASP code and the resulting data were imported into the Phonopy program. The dynamical matrices were calculated from the force constants, and the phonon DOS (PDOS) curves were computed using the Monkhorst-Pack scheme.[37] Hexagonal ice (ice Ih) is in Space group P63/mmc, 194; analogous to β-tridymite silica or lonsdaleite, having a six-fold screw axis (rotation around an axis in addition to a translation along the axis).[38] It possesses a fairly open low-density structure, where the packing efficiency is low (~1/3) compared with simple cubic (~1/2) or face-centered cubic (~3/4) structures. In this atomic arrangement, all molecules experience identical molecular environments. The directional dependent PDOS where computed along (001), (010) and (100).[39]

The simulated structure of hexagonal ice is presented in Fig. 2.
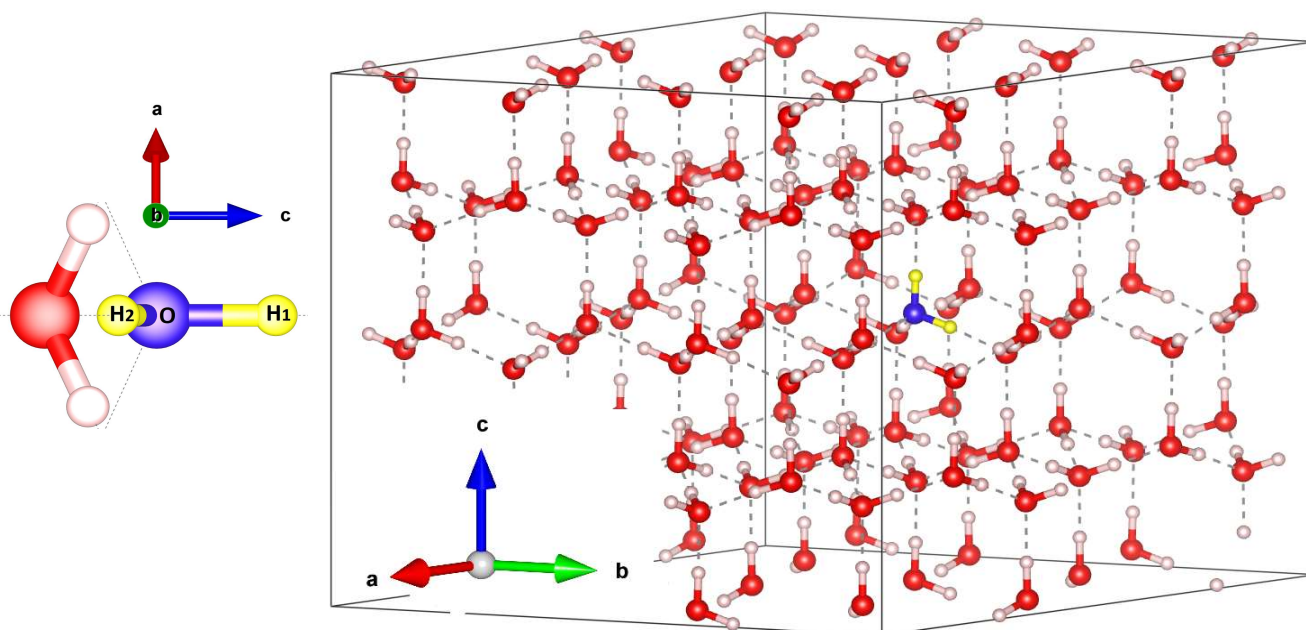
Fig. 2 Simulated structure of ice Ih (O-red, H-white). The blue/yellow colored H_2O represents a crystalline molecule which is oriented relative to the crystallographic axes as in the left inset: OH_1 bond $\parallel$ c, H_1OH_2 molecular plane parallel to the (b,c) plane, a $\perp$ molecular plane (shown for clarity in the left inset for a b direction view). The current Ke(H) analysis refers to the Cartesian components of the H_1-VDOS according to the directions of Fig. 1.

Results and Discussion

Fig. 3 depicts the calculated Cartesian components of the H_1-VDOS in ice Ih. Fig. 4 compares the directional partial VDOS of the two protons in H_2O. In the two figures the Cartesian directions correspond to H_2O molecular orientation as defined in Fig. 1.
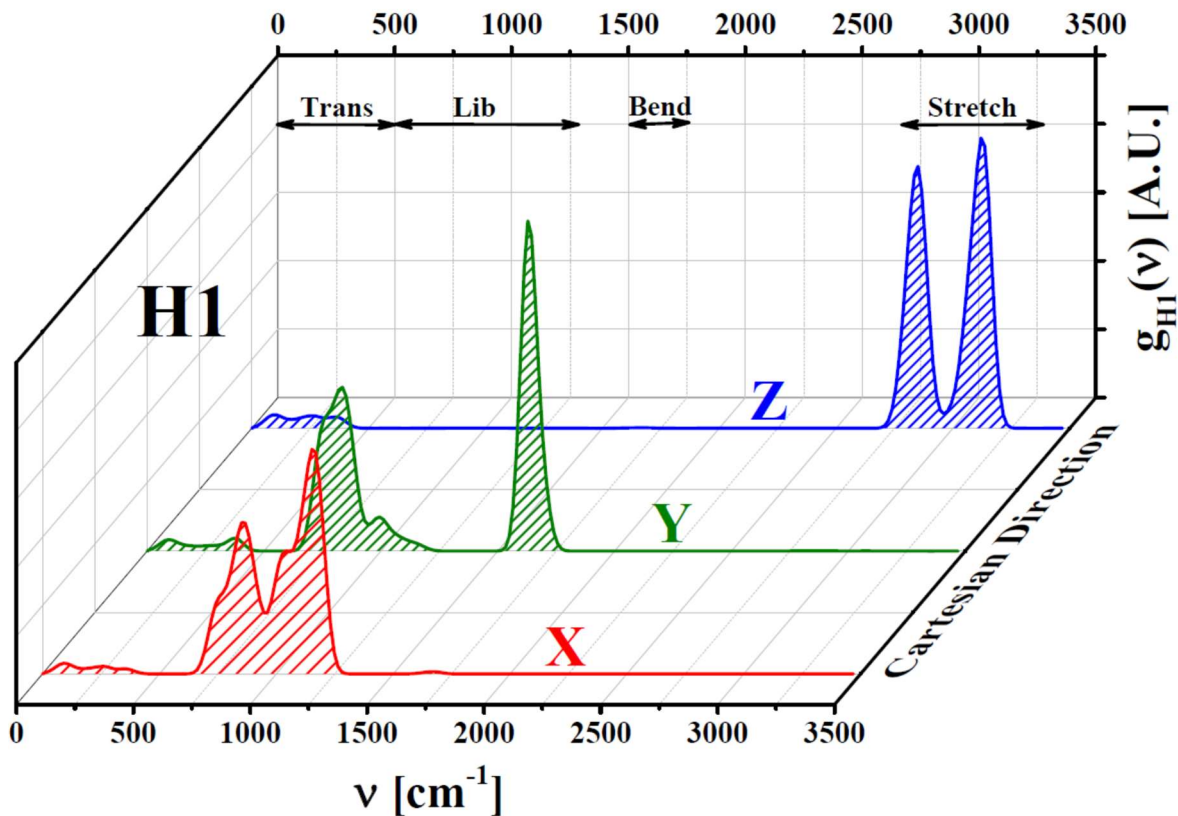
Fig. 3 Calculated Cartesian components (X -red, Y-green, Z-blue) of the H1-VDOS, $g_{H1}(\upsilon)$. Assignments of phonon bands to H_2O lattice (translation and libration) and internal (bending and stretching) are indicated.

Figs. 3 and 4 provide a clear view of the strong anisotropy of the protons VDOS in H_2O. Overall, the anisotropies emerging from those Figures fully comply with the relative orientations between the two OH bonds in the chosen XYZ axes system (Fig. 1). It may first

be noted in Fig. 4 that while the translational phonon band (0-500 cm^{-1}) of either proton along the three Cartesian directions are practically the same (nearly isotropic translational VDOS), all remaining bands, of libration (630-1330 cm^{-1}), bend (1500-1750 cm^{-1}) and stretch (2700-3500 cm^{-1}), possess markedly different intensities along each direction in accord with the protons movements. Accounting for the stretch bands in Fig.3 for example, H$_1$ which vibrates along OH$_1$ that is directed along Z, possess high intensity phonons (solid blue lines in Fig. 3) compared to nearly zero intensities along the X and Y directions (solid red and green lines in Fig. 3 respectively).
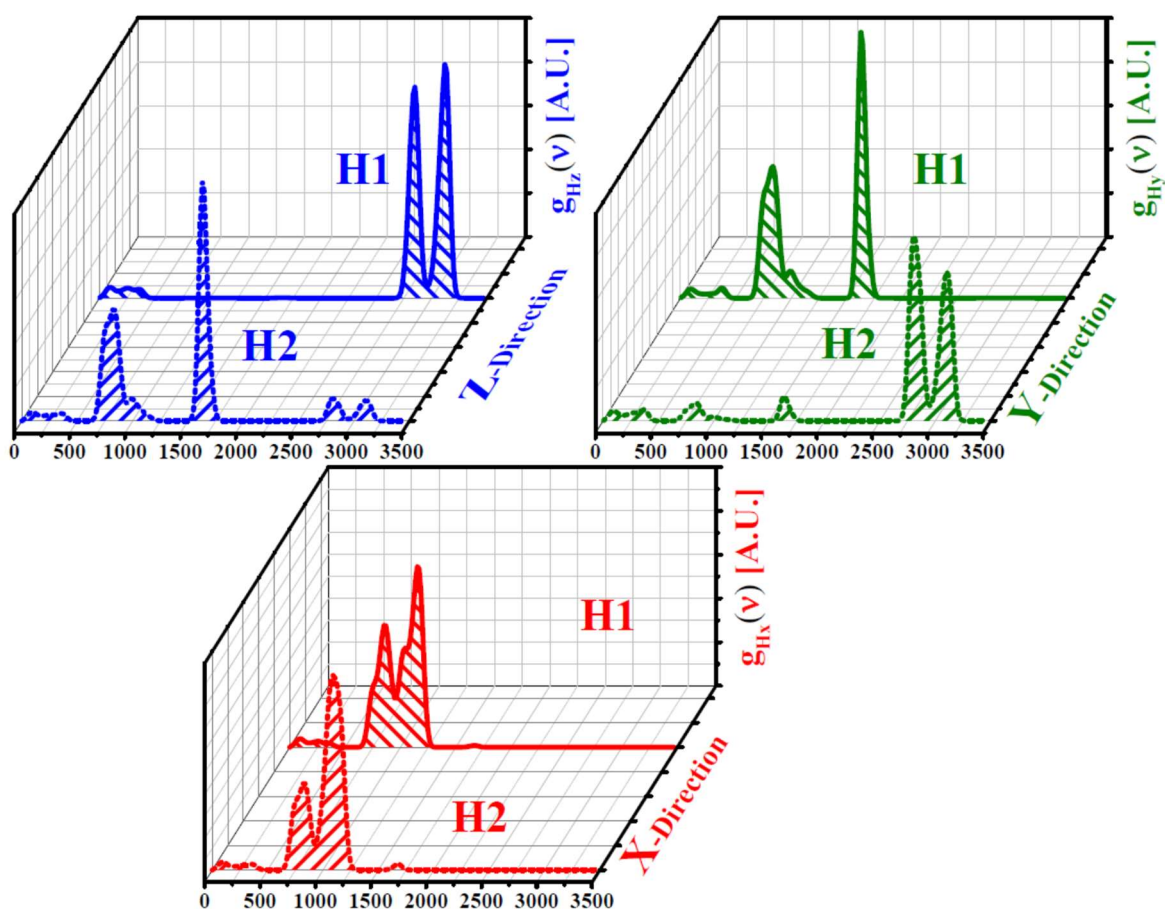
Fig. 4 Calculated Cartesian components (X -red, Y-green, Z-blue) of the H1- (solid) and H2- (dotted) VDOS. Abscissa value are frequencies in cm^{-1} units.

As for the H$_2$ atom whose OH$_2$ bond is perpendicular to X and nearly normal to Z (aligned by ~ 17° with respect to Y), it exhibits mostly a large Y VDOS component along the stretch

band and a much smaller Z component (Fig. 4). Along the X direction, being normal to the H_2O plane, both protons have negligible X stretch components (Fig. 4). It may be also expected that both protons have comparable librational and nearly zero bend intensities along X, while along Y those of H_2 are by far larger than those of H_1. All those features may be easily understood by a consideration of Fig. 1.

The above VDOS calculation may also be validated by accounting for: (1) the *total* H_2O-VDOS $\sum_l [g_{H_{1l}}(\upsilon) + g_{O_l}(\upsilon) + g_{H_{2l}}(\upsilon)]$ from which the averages of the five fundamental frequencies (weighted by $g_{H_2O_l}(\upsilon)$) may be extracted, and (2) the averaged energy fractions shared by the proton, $[g_{H_{1l}}(\upsilon) + g_{H2_l}(\upsilon)]/2$, in each fundamental energy band of the total H_2O-VDOS. The results (summarized in Table I) may then by compared to the experimental frequencies of H_2O and to the SE calculated energy fractions.

Table I Averaged frequencies (υ_j) of the five fundamental modes of motion of H_2O and their corresponding kinetic energy fractions (S_j) shared by the protons. The calculated (*p*VDOS) frequencies and energy fractions are compared to experimental and SE results respectively.

υ_j [cm^{-1}]		S_j	
*p*VDOS	Experiment	*p*VDOS	SE
223	207	0.048	0.056
950	782	0.481	0.475
1641	1650	0.159	0.153
2833	3085	0.157	0.154
3101	3220	0.158	0.159

It may be seen from Table I that the calculated average frequencies differ by 10% at most while those of libration present a ca. 22 % deviation. As for the energy fractions, they differ by 4% at most, with the only exception of the translational fractions which differ by 14 %. The above two large differences may be understood by accounting for the wide ranges of reported librational and translational frequencies in ice which easily cover the above two deviations; these facts support the validity of the above calculation.

The calculated Cartesian components of the H1-, H2- and O-VDOS were used as input data in Eq. 4 for deducing their KE components, $Ke_l(H, O)$. The results are given in Table II.

9

Table II. Deduced $Ke_l(A)$ (l = x, y, z ; A = H_1, O, H_2) values at 0 and 271 K in meV units. $Ke_{tot}(A) = \sum_{l=x,y,z} Ke_l(A)$ refer to the total (isotropic) KE value.

$Ke_l(A)$	H_1OH_2					
	ZPKE			271 K		
l	H_1	H_2	O	H_1	H_2	O
X	30.3	30.6	8.1	30.9	31.2	14.3
Y	36.7	80.5	13.9	37.4	80.9	19.4
Z	87.3	42.8	14.3	87.7	43.4	20.0
$Ke_{tot}(A)$	154	154	36.3	156	155.5	53.7

The KE values reveal the VDOS anisotropy. The first feature to be noted in Table I is that the total (isotropic) KE values of both H_1 and H_2 are practically the same (~155 ±1 meV), regardless of their differently oriented OH bonds. Nonetheless, their Cartesian components are clearly different. Note also that their ZPKE values are smaller by only ~1% compared to the total values at 271K, a direct result of the huge (~ 99%) zero point contribution to Ke(H). The calculated value of Ke(O) is also in very good agreement with experiment and its zero point part is also fairly large (~ 67%), however not as huge as that of the lighter proton.

By accounting for the five characteristic phonon bands of the H_1-VDOS in ice (Fig. 3), the relative contributions of each Cartesian component of each mode of motion to Ke(H_1) were deduced. The results are presented in Fig. 5 together with the total shares of each mode in Ke(H_1). Fig. 5 provides a clear mapping of the vibrational interplay underlying Ke(H_1); here again, the results are in full accordance with the chosen molecular orientation (Fig. 1): all translational components contribute equally and negligibly to Ke(H_1). The stretching part of Ke(H_1) is contributed only by the Z component of the H_1-VDOS. The H_2O bending part arise only from the Y component of the H_1-VDOS (meaning that the internal modes only contribute to the H_2O planar motion, the X component of Ke(H_1) is contributed mainly by the out-of-plane libration of H_2O around the Y-axis. Finally, the libration of H_2O around Z (the OH_1 direction) has no contribution to Ke(H1).
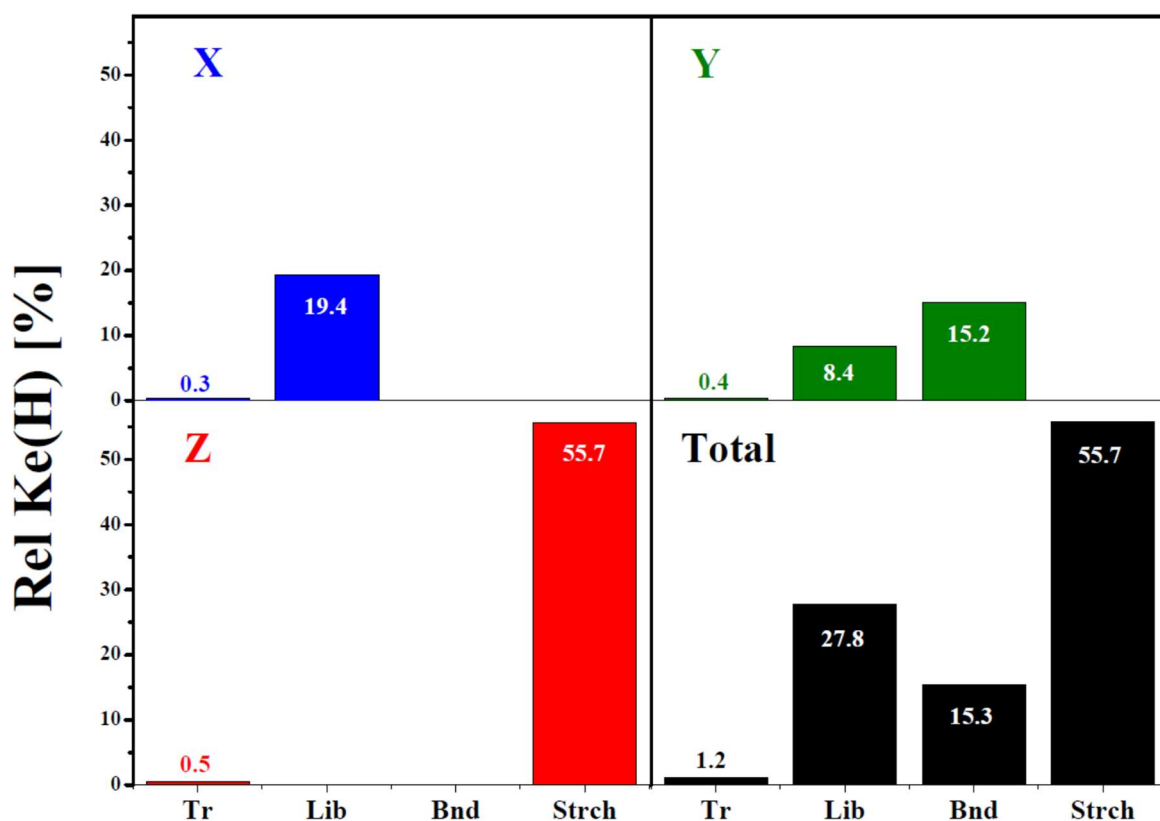
Fig. 5 Fractional fundamental parts of Ke (H1) and of its Cartesian components.

Such a rich informative mapping of the Ke(H) anisotropy could be highly valuable in exploring quantum competing effects such as those reported by DINS to occur upon melting of heavy water.[5] It was reported in Ref. 5 that upon transition from the liquid to the solid, the DINS data show substantial increase in $Ke_x(D)$ (associated with motion normal to the D_2O plane) accompanied with a corresponding large decrease in $Ke_z(D)$ (associated with motion parallel to the covalent O−D bond). The opposite changes in those KE components, which lead to a much smaller change in the total kinetic energy, were viewed as a signature of CQEs in Ke(H). Here, the more hindered librations in the solid phase and the weakening of the covalent bond, are consistent with the red shift of the stretch peak observed in ice. A pVDOS analysis of liquid and solid D_2O can thus provide a direct detailed measure for the above effect.

Comparison with experiment

It should first be noted that the two protons of H_2O (Fig. 1) are *distinguishable* in terms of the relative orientation of their OH bonds with respect to the XYZ Cartesian directions.

Note also that the molecular orientation in Fig. 1 was chosen so that the resulting KE components provide a direct comparison with experimental data. Moreover, in DINS experiments on *isotropic* samples, such as ice and liquid water, the neutron momentum distribution, $n_H(p)$, depends only on the proton momentum along the q direction. Here, the Cartesian components of Ke(H) are extracted from the measured neutron Compton profile, NCP, by assuming that $n_H(p)$ arises from a *spherical average* of an anisotropic Gaussian distribution involving the three Cartesian variances of the total NCP. Differently from the above, in the *p*VDOS approach, the Cartesian Ke(H) components are first calculated from which the mean value is then deduced.

Only two reports are available in the literature regarding the Cartesian components of the proton kinetic energy in light ice. These include DINS[2,8] and INS[2] studies, both treating Ke(H) along and perpendicular to the OH bond at 271 K. The calculated and measured results are presented in Table III and Fig. 6.

Table III. Calculated and measured Ke(H) Cartesian components of ice Ih at 271 K.

$Ke_i(H_1)$	Calc.			Exp.	
	DFT	SE		DINS[8]	DINS[2]
	H-VDOS	INS[2]	This study		
X	30.9	21.6 ±0.3	23 ± 3	28 ± 2	29 ± 2
Y	37.4	34.4 ± 1.2	36 ± 3	38 ± 5	38 ± 3
Z	87.7	98.8 ± 1.2	93 ± 3	91 ± 5	87 ± 3
$Ke_{tot}(A)$	156	154 ± 2	152 ± 3	157 ± 2	154 ± 2
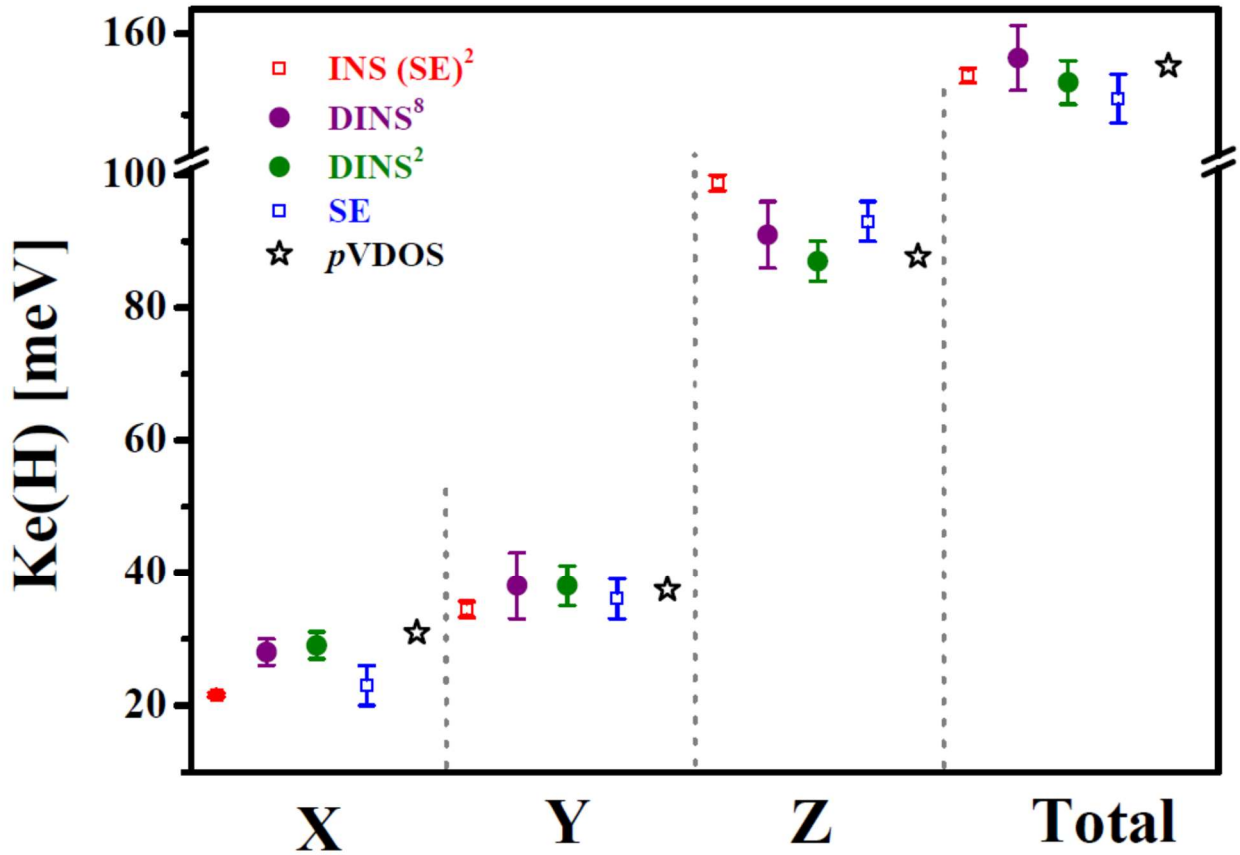
Fig. 6 Current SE and DFT-*p*VDOS calculated values of the total Ke(H) and its Cartesian components versus published INS and DINS results.

Table III and Fig. 6 show that there is a very good agreement between the DINS measured values and the DFT calculation of the Cartesian components and also of the total Ke(H). However a relatively large deviation occurs from the SE results; this may be attributed to the uncertainties in the experimental translation and libration H_2O frequencies used as input data. The above results emphasize the importance of the accuracy provided by the *p*VDOS approach, because CQEs and NQEs that are considered as key effects underlying the behavior of Ke(H), can be very small and may thus be captured only by using the DFT-*p*VDOS calculations. Another important advantage of the *p*VDOS approach is its great success in predicting the DINS Ke(H) value of nano-confined H_2O, e.g. in Beryl, while the SE approach entirely failed to do so.[30]

Conclusions

We report on the first DFT calculation of the Cartesian components of the partial H-VDOS in light ice, from which the components of the proton kinetic energy along and normal to the hydrogen bond were deduced. The results revealed a very good agreement with DINS measurements and were better than those obtained using the SE method. However, the two methods were both successful in treating *pure* H_2O phases. Another advantage of applying the *p*VDOS over SE is that it can predict the Cartesian components of Ke(H) thus providing a valuable tool for explaining signatures of CQEs and nuclear quantum effects (NQEs) in H_2O phases and its vibrational dynamics. The main advantage of the *p*VDOS over SE was revealed in deducing the Ke(H) value in nanoconfined water for which the SE approach was invalid.

References

[1] Y. Finkelstein and R. Moreh, Chem. Phys. **431–432**, 58 (2014).

[2] C. Andreani, G. Romanelli, and R. Senesi, Chem. Phys. **427**, 106 (2013).

[3] Y. Finkelstein and R. Moreh, Curr. Phys. Chem. **7**, 3 (2017).

[4] a. Parmentier, J.J. Shephard, G. Romanelli, R. Senesi, C.G. Salzmann, and C. Andreani, J. Phys. Chem. Lett. **6**, 2038 (2015).

[5] G. Romanelli, M. Ceriotti, D.E. Manolopoulos, C. Pantalei, R. Senesi, and C. Andreani, J. Phys. Chem. Lett **4**, 3251 (2013).

[6] M. Ceriotti and D.E. Manolopoulos, Phys. Rev. Lett. **109**, 100604 (2012).

[7] G. Romanelli, R. Senesi, X. Zhang, K.P. Loh, and C. Andreani, Phys. Chem. Chem. Phys. **17**, 31680 (2015).

[8] C. Andreani, G. Romanelli, and R. Senesi, J. Phys. Chem. Lett. **7**, 2216 (2016).

[9] G. Romanelli, F. Fernandez-Alonso, and C. Andreani, J. Phys. Conf. Ser. **571**, 012003 (2014).

[10] R. Moreh and D. Nemirovsky, J. Chem. Phys. **131**, 054305 (2009).

[11] R. Moreh and D. Nemirovsky, J. Chem. Phys. **130**, 174303 (2009).

[12] R. Moreh and Y. Finkelstein, Phys. Rev. B **61**, 7700 (2000).

[13] R. Moreh, Y. Finkelstein, and H. Shechter, Phys. Rev. B **53**, 16006 (1996).

[14] R. Moreh, H. Pinto, Y. Finkelstein, V. Volterra, Y. Birenbaum, and F. Beguin, Phys. Rev. B **52**, 5330 (1995).

[15] Y. Finkelstein, O. Beck, R. Moreh, D. Jäger, U. Kneissl, J. Margraf, H. Maser, and H.H. Pitz, Phys. Rev. B **58**, 4166 (1998).

[16] R. Moreh, O. Beck, D. Jäger, Y. Finkelstein, U. Kneissl, J. Margraf, H. Maser, and H. Pitz, Phys. Rev. B **56**, 187 (1997).

[17] O. Beck, Y. Ruf, Y. Finkelstein, M. Cardona, T.R. Anthony, D. Belic, T. Ecket, D. Jager, U. Kneissl, H. Masser, R. Moreh, A. Nord, H.H. Pitz, and A. Wolpert, J. Appl. Phys. **83**, 5484 (1998).

[18] Y. Finkelstein, R. Moreh, S.L. Shang, Y. Shchur, Y. Wang, and Z.K. Liu, J. Chem. Phys. **144**, 054302 (2016).

[19] R. Senesi, A. Pietropaolo, A. Bocedi, S. Pagnotta, and F. Bruni, Phys. Rev. Lett. **98**, 138102 (2007).

[20] A. Pietropaolo, D. Fernandez-Cañoto, E. Perelli-Cippo, S. Dirè, and P. Prosposito, Phys. Rev. B - Condens. Matter Mater. Phys. **77**, 014202 (2008).

[21] V. Garbuio, C. Andreani, S. Imberti, A. Pietropaolo, G.F. Reiter, R. Senesi, and M.A. Ricci, J. Chem. Phys. **127**, 154501 (2007).

[22] G.F. Reiter, A.I. Kolesnikov, S.J. Paddison, P.M. Platzman, A.P. Moravsky, M.A. Adams, and J. Mayers, Phys. Rev. B **85**, 045403 (2012).

[23] A.I. Kolesnikov, G.F. Reiter, N. Choudhury, T.R. Prisk, E. Mamontov, A. Podlesnyak, G. Ehlers, A.G. Seel, D.J. Wesolowski, and L.M. Anovitz, Phys. Rev. Lett. **116**, 167802 (2016).

[24] J. a Morrone, V. Srinivasan, D. Sebastiani, and R. Car, J. Chem. Phys. **126**, 234504 (2007).

[25] C.P. Herrero and R. Ramirez, Chem. Phys. **461**, 125 (2015).

[26] C.P. Herrero and R. Ramirez, J. Chem. Phys. **137**, 104505 (2012).

[27] R. Ramirez and C.P. Herrero, Phys. Rev. B - Condens. Matter Mater. Phys. **84**, 064130 (2011).

[28] a. Parmentier, J.J. Shephard, G. Romanelli, R. Senesi, C.G. Salzmann, and C. Andreani, J. Phys. Chem. Lett. **6**, 2038 (2015).

[29] A. Striolo, A.A. Chialvo, K.E. Gubbins, and P.T. Cummings, J. Chem. Phys. **122**, 234712 (2005).

[30] Y. Finkelstein, R. Moreh, S.L. Shang, Y. Wang, and Z.K. Liu, J. Chem. Phys. **146**, 124307 (2017).

[31] C. Andreani, M. Krzystyniak, G. Romanelli, R. Senesi, and F. Fernandez-alonso, Adv. Phys. **65**, 1 (2017).

[32] Y. Finkelstein and R. Moreh, J. Chem. Phys. **139**, 044716 (2013).

[33] G. Kresse and J. Furthmiiller, Comput. Mater. Sci. **6**, 15 (1996).

[34] G. Kresse and J. Furthmu, Phys. Rev. B **54**, 11169 (1996).

[35] J.P. Perdew, K. Burke, and M. Ernzerhof, Phys. Rev. Lett. **77**, 3865 (1996).

[36] A. Togo and I. Tanaka, Scr. Mater. **108**, 1 (2015).

[37] H.J. Monkhorst and J.D. Pack, Phys. Rev. B **13**, 5188 (1976).

[38] T. Ikeda-fukazawa, S. Horikawa, T. Hondoh, and K. Kawamura, J. Chem. Phys. **117**, 3886 (2002).

[39] Https://atztogo.github.io/phonopy/setting-tags.html#projection-direction-tag